Q. J. R. Meteorol. Soc. (2004), **130**, pp. 1349–1372 doi: 10.1256/qj.03.40

A canopy model of mean winds through urban areas

By O. COCEAL* and S. E. BELCHER
University of Reading, UK

(Received 3 March 2003; revised 24 September 2003)

SUMMARY

An urban canopy model is developed for spatially averaged mean winds within and above urban areas. The urban roughness elements are represented as a canopy-element drag carefully formulated in terms of morphological parameters of the building arrays and a mean sectional drag coefficient for a single building. Turbulent stresses are represented using a mixing-length model, with a mixing length that depends upon the density of the canopy and distance from the ground, which captures processes known to occur in canopies. The urban canopy model is sufficiently simple that it can be implemented in numerical weather-prediction models.

The urban canopy model compares well with wind tunnel measurements of the mean wind profile through a homogeneous canopy of cubical roughness elements and with measurements of the effective roughness length of cubical roughness elements. These comparisons give confidence that the basic approach of a canopy model can be extended from fine-scale vegetation canopies to the canopies of large-scale roughness elements that characterize urban areas.

The urban canopy model is also used to investigate the adjustment to inhomogeneous canopies. The canonical case of adjustment of a rural boundary layer to a uniform urban canopy shows that the winds within the urban canopy adjust after a distance $x_0 = 3L_c \ln K$, where L_c is the canopy drag length-scale, which characterizes the canopy-element drag, and $\ln K$ depends weakly on canopy parameters and varies between about 0.5 and 2. Thus the density and shape of buildings within a radius x_0 only determine the local canopy winds. In this sense x_0 gives a dynamical definition of the size of a neighbourhood.

The urban canopy model compares well with observations of the deceleration of the wind associated with adjustment of a rural boundary layer to a canopy of cubical roughness elements, but only when the sectional drag coefficient is taken to be somewhat larger than expected. We attribute this discrepancy to displacement of streamlines around the large-scale urban roughness elements, which yields a stress that decelerates the wind. A challenge for future research is to incorporate this additional 'dispersive stress' into the urban canopy model.

KEYWORDS: Atmospheric boundary layer Urban canopy model Urban meteorology

1. INTRODUCTION

Mixing and transport within urban areas is important for a number of applications. Urban areas exert enhanced drag on the boundary layer above, which may have an effect on mesoscale weather processes (e.g. Craig and Bornstein 2002). At the other end of the scale, local winds within urban areas form part of local weather forecasts and are required for building design applications (e.g. Panofsky and Dutton 1984). In addition, urban air quality is becoming an issue of increasing concern (Vardoulakis *et al.* 2003). The mixing and transport of pollutants in urban areas is controlled by processes that range from the street scale, through the neighbourhood scale, up to the city scale and beyond (Britter and Hanna 2003). A modelling system to forecast urban air quality must therefore be based upon a dynamical model that accounts for the mixing and transport processes through this wide range of scales. These applications motivate the need to find an efficient methodology to calculate the mean winds and turbulence in and above urban areas within numerical weather prediction (NWP).

The dynamical effect of urban areas is usually represented in NWP at present through a simple roughness length. But this approach gives no information on the mixing and transport within the urban canopy. In addition, a roughness length can be defined only when the wind profile near the surface is logarithmic. When the density of the roughness elements varies over short length-scales the boundary-layer flow constantly evolves, and it may not be possible to even define a roughness length (Cheng and

* Corresponding author: Department of Meteorology, University of Reading, Reading, Berkshire RG6 6BB, UK.
e-mail: o.coceal@reading.ac.uk

Castro 2002a). The same issue undoubtedly frustrates attempts to measure the roughness length of urban areas, and may explain the wide scatter in measurements reported by Grimmond and Oke (1999). At the same time it is not practical, and probably not desirable, to compute the flow around every building in a large city such as London, because such an approach would require exhaustive data on building geometry and astronomical computer power. What is required then is a more sophisticated method of representing the dynamical effects of urban areas than a roughness length, that (i) gives estimates for the mean winds and turbulence within the urban area, (ii) does not depend on a logarithmic wind profile and (iii) is simple enough to be affordable in NWP.

This paper describes an *urban canopy model*, which provides a methodology that satisfies these requirements. The idea underlying the urban canopy model is to represent the roughness elements within the urban area as a porous medium which is permeable to the air flow. The focus is on the wind representative of a spatial area: we aim to calculate the spatially averaged wind velocity. Now, each roughness element exerts a resistive force, or drag, on the local air flow, whose effect on the spatially averaged wind is represented here as a body force spread smoothly through the urban canopy region. The strength of this approach is that it avoids the unnecessary detail, and huge cost, of resolving the flow around each individual building, but it does capture the variations in the mean wind as the density of the buildings changes. In this sense the urban canopy model resolves neighbourhood variations in the mixing and transport.

This general approach has been developed for flow through fine-scale roughness elements, such as in vegetation canopies (see the recent excellent review by Finnigan (2000)). Intuitively, this porous medium approach is expected to be well suited to canopies of fine-scale roughness elements, where there is a separation of scales between the size of the canopy roughness elements and the canopy itself. Simple distributed drag models of urban areas have been proposed in the literature (e.g. Brown 2000, Martilli *et al.* 2002). But urban areas have large-scale roughness elements, which do not obviously have the separation of scales, and so the basic approach remains to be validated. Nor have previous formulations for urban areas been rigorously based and so they may miss important processes. Finally, the dynamical implications of an urban canopy model have yet to be fully explored. Further aims of this paper are therefore to develop an urban canopy model with parametrizations suitable for large-scale urban roughness elements, and to validate this urban canopy model using wind-tunnel and field data for flow through large-scale roughness elements.

The urban canopy model is formulated in section 2. The model contains parametrizations for the turbulent mixing and the canopy-element drag that are carefully chosen using results from wind-tunnel measurements with arrays of large-scale urban-like roughness elements. In section 3 the urban canopy model is used to calculate the flow produced when the atmospheric boundary layer has adjusted to a very long homogeneous urban canopy. The results are compared with wind-tunnel measurements. In section 4 the urban canopy model is used to examine the adjustment of a rural boundary layer to an urban canopy. Belcher *et al.* (2003) (hereafter BJH) developed a quasi-linear canopy model for this process. In the present paper the fully nonlinear dynamical equations are solved numerically, to provide a more flexible model. The calculations are compared with observations. Finally, conclusions are offered in section 5.

2. Formulation of the urban canopy model

The urban canopy model is formalized by averaging the governing equations, firstly over time, as is always done in turbulent boundary-layer flows, and secondly over a

volume (Raupach and Shaw 1982; Finnigan 2000). The averaging volume is taken to be very thin in the vertical, and large enough in the horizontal to include a number of canopy elements, but not so large as to lose any spatial variation in the density of canopy elements. If the canopy is a periodic array of elements, then the averaging volume is taken to be the repeating unit. For a real urban area, with varying building density, we assume therefore a scale separation between the spacing of individual buildings over which the averaging is performed, and the variations in building density, which is resolved by the model. The spatial average is then effectively a horizontal average and yields vertical profiles of flow variables.

Under the two operations of time and space averages, prognostic variables then have three components, which for the streamwise velocity u are

$$u = U + \widetilde{u} + u'. \tag{1}$$

Here $U = \langle \overline{u} \rangle$ is the time- and space-averaged velocity, referred to here as the mean velocity, $\widetilde{u} = \overline{u} - U$ is the spatial variation of the time-mean flow around individual roughness elements, $u' = u - U - \widetilde{u}$ is the turbulent fluctuation, and overbar denotes time average and angle brackets denote spatial average.

The aim is to calculate the mean wind vector $U_i(x, y, z)$, which is obtained by solving the time- and space-averaged momentum equations, which following Raupach and Shaw (1982) and Finnigan (2000) are

$$\frac{\mathrm{D}U_i}{\mathrm{D}t} + \frac{1}{\rho}\frac{\partial P}{\partial x_i} = -\frac{\partial}{\partial x_j}\langle \overline{u_i' u_j'} \rangle - \frac{\partial}{\partial x_j}\langle \widetilde{u}_i \widetilde{u}_j \rangle - D_i. \tag{2}$$

The averaging procedure thus produces three new terms in the momentum equation. There is a spatially averaged *Reynolds stress* $\langle \overline{u_i' u_j'} \rangle$, which represents spatially averaged momentum transport due to turbulent-velocity fluctuations; there is a *dispersive stress* $\langle \widetilde{u}_i \widetilde{u}_j \rangle$, due to momentum transport by the spatial deviations from the spatially averaged wind; and finally, within the canopy volume, there is a smoothly varying *canopy-element drag* D_i, which arises from spatially averaging the localized drag due to individual roughness elements.

There is experimental evidence (Finnigan 1985; Cheng and Castro 2002b) that near the top of the canopy the dispersive stress is very small compared to the Reynolds stress. The dispersive stress may be a larger fraction near the bottom of the canopy (Bohm *et al.* 2000), but both stresses tend to be small there. Hence, as we shall see, the drag term is important through the whole volume of the canopy, whereas the dispersive stress can be neglected; although we shall see in section 4 that the finite volumes of the canopy elements lead to a dispersive stress that is important upwind of the canopy.

In the present model, the dispersive stress is therefore neglected. The urban canopy model is completed on parametrizing the drag and the turbulent stress. These aspects are described next.

(*a*) *Parametrization of the canopy-element drag*

In the averaged momentum equation (2) the canopy-element drag D_i arises through spatially averaging the localized drag due to individual canopy elements. The canopy-element drag is a body force per unit volume on the spatially averaged flow and can be related to the drag of an individual canopy element in the following way. Consider an array of N obstacles each with frontal area A_f, height h and drag coefficient $c_d(z)$, distributed over a total averaging area A_t. The force acting at height z on each element is $1/2\rho U^2(z) c_d(z) A_\mathrm{f}\, \mathrm{d}z/h$. (Notice how the engineering convention is followed here

with the drag coefficient defined including a factor of half.) The thin averaging volume at height z is given by $(1-\beta)A_t\,\mathrm{d}z$, where $(1-\beta)$ is the fractional volume occupied by air in the canopy. Hence, the total force per unit volume acting on the air at height z is

$$\rho D_i = \frac{1}{2}\rho \frac{c_d(z)\sum A_f}{hA_t(1-\beta)}|U|U_i. \tag{3}$$

The *roughness density* $\lambda_f = \sum A_f/A_t$ is the total frontal area per unit ground area, and hence expresses a measure of the packing density of the obstacles (e.g. Wooding *et al.* 1973). The canopy-element drag can then be expressed as

$$D_i = \frac{1}{2}\frac{c_d(z)\lambda_f}{h(1-\beta)}|U|U_i = \frac{|U|U_i}{L_c}, \tag{4}$$

where the *canopy drag length-scale* L_c is defined by

$$L_c = \frac{2h}{c_d(z)}\frac{(1-\beta)}{\lambda_f}. \tag{5}$$

This canopy drag length-scale is a fundamental dynamical length-scale of the canopy, as we shall see. The illustrative breakdown presented shows that L_c is determined by the geometry and layout and the obstacles, as expressed by the parameters λ_f, β and $c_d(z)$. The drag coefficient $c_d(z)$ has a dependence on the shape of the obstacles. If different shapes of obstacles are present in an averaging volume then the $c_d(z)$ that appears in the equations represents a mean value. For urban areas it is appropriate to think of canopy elements, i.e. buildings that have a horizontal cross-section that is uniform with height. The canopy volume may be defined as hA_t, where h is the plan area weighted average building height $h \equiv \sum hA_p/\sum A_p$, and A_p is the plan area of an individual building. Then simple geometry shows that the volume fraction β occupied by the buildings is equal to the plan area density λ_p, defined as the total plan area per unit ground area: $\lambda_p = \sum A_p/A_t$. Hence, the canopy drag length-scale L_c can be calculated from the morphological parameters λ_f, λ_p and h together with the drag coefficient $c_d(z)$. For an array of cubes $\lambda_f = \lambda_p \equiv \lambda$.

It is important to appreciate that $c_d(z)$ is the *sectional drag coefficient* that relates the drag at height z to the average wind speed at that height (Macdonald 2000). The sectional drag coefficient differs from the, conventionally used, depth-integrated drag coefficient C_{dh}, which is defined to relate the total drag force F_D, acting over the whole depth of the canopy element, to the mean wind speed at one particular height. When this height is taken to be the top of the canopy element $z = h$, this definition yields

$$F_D = \tfrac{1}{2}\rho C_{dh} U_h^2 A_f. \tag{6}$$

In contrast, D defined in (3) is the drag per unit volume of air. The values of $c_d(z)$ and C_{dh} are very different as we shall see. To determine $c_d(z)$ in practice requires knowledge of the spatially averaged wind profile and the vertical profile of the drag within the canopy. In the next subsection, recent wind-tunnel data for the flow within an array of cubical obstacles is used to estimate $c_d(z)$.

(*b*) *Estimation of the sectional drag coefficient*

In order to completely determine the model it is necessary to prescribe $c_d(z)$. It is not appropriate to use values for the depth-integrated drag coefficient C_{dh}, which has been measured many times. Instead, as explained above, the urban canopy model depends upon the sectional drag coefficient, which is not measured routinely.

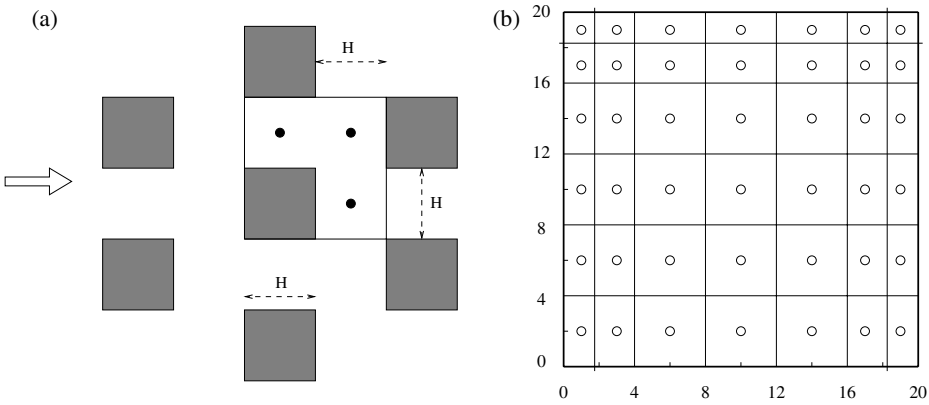

Figure 1. (a) Velocity measurements at positions indicated by dots, and (b) pressure measurements at positions indicated by circles, on the front and back faces of a cube, in experiment of Cheng and Castro (2002b). The numbers in (b) represent distance (mm).

Cheng and Castro (2002b) performed experiments on simulated boundary-layer flow over a staggered array of cubical canopy elements in a wind tunnel. The array had an obstacle density of $\lambda = 0.25$ and was sufficiently extensive for equilibrium conditions to prevail in the test section downstream. In these equilibrium conditions spatial averaging can be performed over a repeating unit such as is shown in Fig. 1(a). Cheng and Castro measured the velocity profiles at the positions indicated by the dots using laser doppler anemometry probes. They also measured the pressure over the front and back of a cube at different positions as indicated in Fig. 1(b). These measurements are used here to compute the drag coefficient profile $c_d(z)$ as follows.

First the velocity and pressure values at each vertical level are averaged over the repeating unit area to yield measures of the spatially averaged mean velocity $U(z)$ and the pressure drop $\Delta p(z)$ across a cube. The sectional drag coefficient $c_d(z)$ is then computed from the following relation:

$$\Delta p(z) = \tfrac{1}{2}\rho U^2(z) c_d(z). \tag{7}$$

The results of this computation are shown in Fig. 2. Unfortunately, the laser doppler anemometry velocity measurements were inaccurate below about half the height h of the cubes because of reflections of the laser beam off the sides of the cubes (Cheng, personal communication), and reliable values for $c_d(z)$ cannot therefore be obtained from these measurements for $z < h/2$. This is reflected in the outlying data point at the height $z = 0.3h$ in Fig. 2. If this last data point is therefore disregarded, it is seen that the sectional drag coefficient increases from a little below 2 at the top of the obstacle to about 3 below $0.75h$, whence it seems to tend to a constant value.

This behaviour is consistent with what would be expected intuitively: smaller values of $c_d(z)$ at the top of the cube arise because air flows both over and around the top of the cube, thus relieving the drag; nearer the base, the air flows only around the cube enhancing the drag. (Note that in analogy the drag coefficient for a cylinder is higher than for a sphere (Batchelor 1967, p. 341).) The observations in Fig. 2 suggest that tall square-section cuboids of height h and breadth b will have $c_d(z) \approx 2$ within a depth of order $0.75b$ of the top, where these end effects occur, and then a constant $c_d(z) \approx 3$ over the remaining depth. For practical purposes, we use here a height-averaged value for the sectional drag coefficient, denoted by $\overline{c}_d$, instead of the full vertical profile $c_d(z)$.

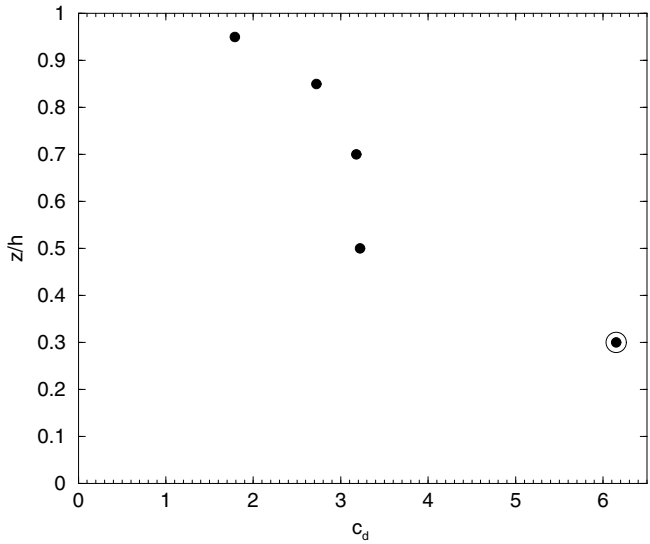

Figure 2. Sectional drag coefficient computed from measurements of Cheng and Castro (2002b). The lowest level is disregarded.

An average value of $\overline{c}_d = 2.6$ can be computed from the above results. This value would be appropriate for use in modelling turbulent shear flow over cubes. For tall cuboids, the end effect becomes a small fraction of the total depth and we expect $\overline{c}_d \approx 3$. This narrow range of typical values for $\overline{c}_d$ constrains the urban canopy model well.

These trends are well supported by data from ESDU (1986), where measured values of the drag coefficient $\overline{C_{dh}}$, based on the depth-integrated mean-squared velocity $\int_0^h U^2(z)\,\mathrm{d}z$, show an increase from about 1.2 for cubes to about 2.8 for tall cuboids. This drag coefficient $\overline{C_{dh}}$ is different from C_{dh} in that it takes into account the vertical velocity profile. Macdonald (2000) shows that a drag coefficient $\overline{C_{dh}}$ defined in this way has a value close to the mean sectional drag coefficient $\overline{c}_d$ used here. The ESDU data refers to an isolated cube in a near logarithmic velocity profile, and gives $\overline{c}_d \approx \overline{C_{dh}} = 1.2$ in that case. We find above that, in the relatively dense array used by Cheng and Castro (2002b), where the velocity profile is not logarithmic, the value of $\overline{c}_d = 2.6$. This gives an idea of the range of variation of the mean drag coefficient $\overline{c}_d$ with ambient mean velocity profile, and hence with canopy density. Again, for practical purposes we take a value of $\overline{c}_d = 2$, which represents an average between the values of 1.2 and 2.6.

With this value of $\overline{c}_d$, (5) reduces to

$$L_\mathrm{c} = \frac{1-\lambda_\mathrm{p}}{\lambda_\mathrm{f}}\, h \tag{8}$$

and therefore L_c is here modelled as a constant length-scale.

(*c*) *Reynolds stress parametrization*

The Prandtl mixing-length model is used here to represent the spatially averaged turbulent stress, namely

$$\langle \overline{u_i' u_i'} \rangle = l_\mathrm{m}^2 |S| S_{ij}, \tag{9}$$

where $S_{ij} = (1/2)(\partial U_i/\partial x_j + \partial U_j/\partial x_i)$ is the shear rate. Here the spatially averaged mixing length l_m represents a spatially averaged turbulence integral length-scale, which

is expected to depend on characteristics of the canopy, such as the obstacle density. The use of the mixing-length model here is justified with three arguments. Firstly, Raupach *et al.* (1996) argue that within homogeneous plant canopies the mean wind profile develops an inflexion point at the top of the canopy, which is then unstable to mixing-layer instability. Large mixing-layer eddies then develop, which dominate the mixing within the canopy, sometimes leading to counter-gradient transport of scalars (Raupach *et al.* 1996). This mixing is observed to lead to an exponential mean wind profile in both vegetation canopies (Finnigan 2000) and canopies of cubical urban-like roughness elements (Macdonald 2000). Such an exponential mean wind profile can be recovered pragmatically by representing the turbulent transport of momentum using a mixing-length model with a constant mixing length. Secondly, Finnigan and Belcher (2003) show that when the canopy is inhomogeneous in the streamwise direction, so that the mean flow is adjusting, the leading-order effect of the turbulent stress on the mean flow can be parametrized using a mixing-length model. Thirdly, the mixing-length model forms the basis of parametrizing turbulence in many numerical weather-prediction models, and so it is a simple and natural choice for this application.

The general form for the spatially averaged mixing length used here is motivated by considering two extreme cases. Firstly, if the canopy is very sparse the turbulence structure of the boundary layer is not much affected by the canopy. The turbulent eddies are, however, blocked by the ground, so that l_m is determined by distance from the ground; thus $l_\mathrm{m} = \kappa z$, where κ is the von Karman constant. Secondly, as argued by BJH, when the canopy is denser the boundary-layer eddies above the canopy are blocked by the strong shear layer that forms near the top of canopy. The mixing length above the canopy is then $l_\mathrm{m} = \kappa(z - d)$, where d is the displacement height of the canopy. Raupach *et al.* (1996) show that the dominant eddies through the depth of a vegetation canopy are then produced from mixing-layer instability of this shear layer at the top of the canopy. The spatially averaged mixing length in the canopy is then expected to be constant with height, say l_c, and to be controlled by the thickness of the shear layer, namely $h - d$. This argues for a constant mixing length in the canopy, $l_\mathrm{c} \propto (h - d)$, when the canopy is dense.

The spatially averaged mixing length for a general canopy is represented here by simply interpolating between these two behaviours of sparse and dense canopies. Since the mixing is constrained by the smaller of the two length-scales, it is appropriate to interpolate using a harmonic mean, namely

$$\frac{1}{l_\mathrm{m}} = \frac{1}{\kappa z} + \frac{1}{l_\mathrm{c}}. \tag{10}$$

Equation (10) also has the attractive feature that, even when the canopy is dense, towards the ground surface $z \ll l_\mathrm{c}$, the spatially averaged mixing length reverts to being controlled by distance from the surface $l_\mathrm{m} \approx \kappa z$. This makes physical sense because the local mixing length near the ground surface is expected to follow $l_\mathrm{m} = \kappa z$ away from regions of recirculating flow. On taking a spatial average, we expect therefore that spatially averaged mixing length will again follow approximately the same form, provided the recirculating flow regions are a small fraction of the whole flow. (We recognize that when the canopy elements become very densely packed the flow near the ground will become dominated by the recirculating flow in wake regions, and this model may not be adequate.) Equation (10) thus yields a spatially averaged mixing length that gives the correct behaviour for both sparse and dense canopies and towards the ground surface.

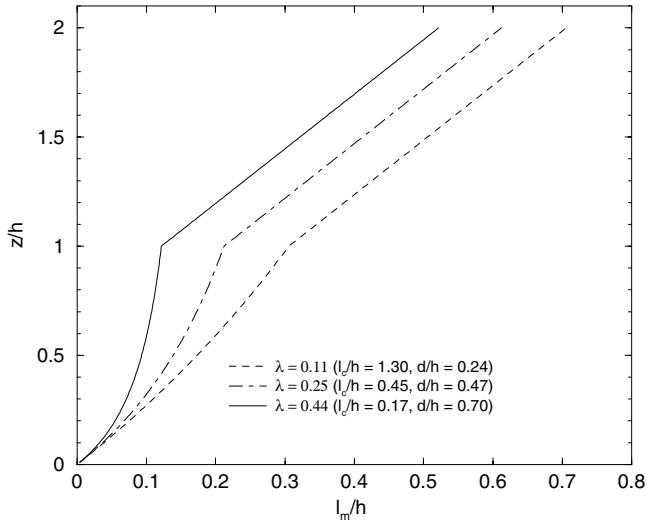

Figure 3. Mixing-length profiles employed in the urban canopy model for different values of the obstacle density λ. Also shown are values of l_c/h, the size of the limiting constant eddy viscosity.

Here, to generate a closed model, l_c is fixed by requiring that at the top of the canopy the mixing length within the canopy is $s\kappa(h-d)$, i.e. a factor s times the mixing length in the boundary layer immediately above the canopy. Hence l_c is determined from

$$\frac{1}{\kappa h}+\frac{1}{l_c}=\frac{1}{s\kappa(h-d)}. \tag{11}$$

We shall find in section 3(a) that the urban canopy model performs well with $s=1$, so that the mixing length is continuous at the top of the canopy.

The turbulence closure is completely specified once d is specified. Based on wind-tunnel data from Hall *et al.* (1998) for regular arrays of cubes, Macdonald *et al.* (1998) proposed the following empirical expression for the ratio d/h as a function of λ_p of the array:

$$\frac{d}{h}=1+A^{-\lambda_p}(\lambda_p-1), \tag{12}$$

where the empirical parameter A is approximately equal to 4. The value $A=4$ is used here. This empirical relationship together with (10) and (11) gives the mixing length l_m within the canopy in terms of the morphological parameters λ_p and h. The mixing length above the canopy is specified to be

$$l_m=\kappa(z-d), \tag{13}$$

which then also ranges correctly from the sparse canopy limit, when $d\approx 0$, to the dense canopy limit, when $d\approx h$.

Figure 3 shows vertical profiles of the mixing length, obtained with $s=1$, for three different canopy densities, $\lambda=0.11$, 0.25 and 0.44, which represent a typical range for an urban area. Also shown are corresponding values of l_c/h, the size of the limiting constant eddy viscosity, to which l_m/h would asymptote in the upper part of a very deep canopy. Here, Fig. 3 shows that l_m, is very different from l_c throughout the depth of the canopy. Hence, the mixing length l_m is not constant with height within the canopy. This reflects an important difference between an urban canopy and a vegetation canopy.

TABLE 1. DETAILS OF SET-UP OF THE SIMULATIONS

Run	Section	Domain size (m)			Grid size			Canopy height, h (m)
		L	W	H	N_x	N_y	N_z	
A	3(a), (b)	–	–	200	1	1	42	2.3
B	4(a)	1000	–	100	130	1	32	2.3
C	4(c), (2D)	1000	–	200	130	1	42	2.3
D	4(c), (3D)	1000	400	100	80	24	42	2.3

See text for explanation of symbols.

Vegetation canopies are generally much deeper, and hence the mixing length in such canopies are constant throughout much of their depth. Note that the displacement–height ratio d/h increases monotonically with λ according to (12). Figure 3 shows how the increase in d with λ affects the mixing-length profile in two ways. Firstly, it reduces the thickness of the shear layer at the top of the canopy $h - d$, which tends to reduce l_c. This means that in the upper portion of denser canopies the mixing length tends to be reduced and constant with height, as in the curve with $\lambda = 0.44$. For sparser canopies l_c is larger and the mixing length is more controlled by the distance from the ground, as in the curve for $\lambda = 0.11$ in Fig. 3. BJH suggest that when $\lambda \ll u_*^2/U_h^2 \approx 0.1$, where u_* is friction velocity, the canopy becomes sparse, in agreement with the model here. Secondly, the increase of d/h with λ tends to sharpen the shear layer, which then becomes more effective in blocking the boundary-layer eddies above the canopy. Thus, the mixing length above the canopy tends to be reduced as the canopy density increases. Hence the turbulence closure used here, whilst simple, reproduces processes known to control mixing in canopies.

(*d*) *Numerical solution of the model equations*

The boundary-layer flow through the urban canopy model is computed here using the Met Office BLASIUS model with the first-order closure modified to accommodate the mixing-length scheme described in section 2(c). The canopy-element drag was also included in the momentum equations within the canopy region. The code then solves the ensemble-averaged momentum, continuity and thermodynamic equations using the anelastic extension of the Boussinesq approximation (Wood 1992; Wood and Mason 1993). All simulations here were performed for conditions of neutral stratification. The boundary conditions are an imposed constant velocity at the top of the domain, and no slip at the bottom. For simulations of flow over a homogeneous canopy, periodic lateral-boundary conditions are used. Simulations of boundary-layer adjustment to a canopy are performed using an inflow boundary condition with a prescribed logarithmic velocity profile, and a zero second derivative outflow boundary condition. The grids are staggered and stretched in all three directions.

The urban canopy model is initialized by specifying the values of the morphological parameters λ_f, λ_p and h and the mean drag coefficient $\overline{c}_d$. These then allow the model parameters L_c, l_c and d to be computed from (5), (11) and (12). The underlying surface roughness z_0 also needs to be specified. Values of λ_f, λ_p and h for typical European and American cities can be found, for example, in Grimmond and Oke (1999).

Table 1 gives details of the set-up of the simulations performed in this paper. Four types of run, denoted by A to D, are performed and the corresponding section in the paper where they are discussed is also indicated. In Table 1, L is the length of the domain in the streamwise direction, W is the domain width and H is the domain height.

The number of grid points in the streamwise, cross-stream and vertical directions are N_x, N_y and N_y, respectively.

3. Flow within and above a homogeneous canopy

If a steady wind blows over a very long, homogeneous, canopy of roughness elements, an internal boundary layer develops above the canopy and sufficiently far downstream the flow fully adjusts to the canopy. In this section we investigate the veracity of the urban canopy model when the flow is adjusted to a homogeneous canopy. First the wind profile within the canopy is compared with wind tunnel measurements analysed by Macdonald (2000). Second the effective roughness of the canopy is calculated with the urban canopy model and compared with wind tunnel measurements analysed by Macdonald *et al.* (1998).

(*a*) *Flow within a homogeneous canopy*

When the canopy is sufficiently extensive the winds both within and above come into streamwise equilibrium: they are adjusted. Within the canopy the dynamical balance is between the vertical stress gradient and the drag force, namely

$$\frac{\partial}{\partial z}\langle\overline{u'w'}\rangle = D_x, \tag{14}$$

where $\langle\overline{u'w'}\rangle = l_{\mathrm{m}}^2(\partial U/\partial z)^2$ and $D_x = U^2/L_{\mathrm{c}}$. For a deep canopy, according to (10), the mixing length is constant with height: $l_{\mathrm{m}} = l_{\mathrm{c}}$. Equation (14) then gives

$$\frac{\partial}{\partial z}\left(\frac{\partial U}{\partial z}\right)^2 = \frac{U^2}{l_{\mathrm{c}}^2 L_{\mathrm{c}}}. \tag{15}$$

Recall that we use a constant, height-independent, L_{c} in the present model. Equation (15) then has an exponential solution (Cionco 1965; Macdonald 2000; BJH)

$$U = U_h\, \mathrm{e}^{(z-h)/l_{\mathrm{s}}}, \tag{16}$$

where U_h is the value of the wind speed at the top of the canopy, $z = h$, and the shear-layer depth (BJH) is

$$l_{\mathrm{s}} = (2l_{\mathrm{c}}^2 L_{\mathrm{c}})^{1/3}. \tag{17}$$

Equations (11) and (12) yield $l_{\mathrm{c}} \propto h$, so that (17) gives $a = h/l_{\mathrm{s}} \propto (h/L_{\mathrm{c}})^{1/3}$. Hence, when the canopy is deep, the dimensionless wind profile, $\hat{U} = U/U_h$, as a function of the dimensionless height $\hat{z} = z/h$, depends on only one parameter, namely L_{c}/h, which defines the density of the canopy. Physically, L_{c} determines the depth into the canopy to which horizontal momentum is mixed before being removed by canopy drag. Hence, L_{c}/h measures this length compared to the depth of the canopy h. When the canopy is sparse, so that the ground surface changes the mixing length and the mean wind profile, there is also a dependence on the roughness length of the ground, through the parameter z_0/h.

The dependence of the normalized, adjusted, wind profile on the parameter L_{c}/h is illustrated in Fig. 4. These wind profiles have been computed using the urban canopy model presented in this paper. The plots confirm that when plotted against $\hat{z}$, $\hat{U}(\hat{z})$ depends only on the value of L_{c}/h. Indeed, profiles for canopies with different values of L_{c} and h, but with the same value of L_{c}/h, collapse onto each other, as shown for

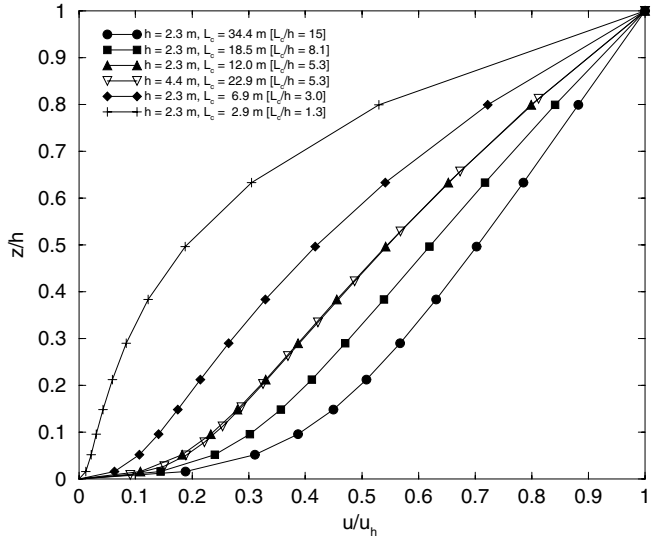

Figure 4. Variation of normalized wind profiles with the canopy density L_c/h. Notice how profiles with the same value of L_c/h collapse onto each other, even if L_c and h differ. The values of roughness density λ were computed from L_c with $\overline{c}_d = 2$. We classify canopies with $L_c/h > 5$ as sparse and canopies with $L_c/h < 5$ as dense. The ratio of underlying surface roughness to canopy height z_0/h is 0.005.

the cases with $h = 2.3$ m, $L_c = 12.0$ m and $h = 4.4$ m, $L_c = 22.9$ m, both of which have the same value of $L_c/h = 5.3$. (Notice the small differences in wind speed near the surface, where the different values of z_0/h play a weak role.) The wind profiles are approximately exponential in the upper part of the canopy, but sparser canopies take on a more logarithmic shape because of the linear mixing length closure near the surface (10). This is shown by the curve with $L_c/h = 15$, which corresponds to $\lambda_f = 0.0625$. Hence, the full solution is sufficiently flexible that it agrees with the analytical solution for dense canopies, while yielding the correct behaviour in the sparse limit. Figure 4 also suggests that canopies with $L_c/h > 5$, which corresponds to $\lambda < 0.15$ if $\overline{c}_d = 2$, are *sparse* and canopies with $L_c/h < 5$, which corresponds to $\lambda > 0.15$ if $\overline{c}_d = 2$, are *dense*. Interestingly, most urban areas are then sparse (and hence the exponential solution does not apply), whereas forest canopies are usually dense (and hence the exponential solution does apply).

Macdonald (2000) used vertical profiles of the horizontal wind speed through a canopy of cubes measured in a wind tunnel by Macdonald *et al.* (1998) to calculate a vertical profile of the spatially averaged wind. He then showed that the spatially averaged wind profiles can be approximated reasonably well by the exponential profile (16) provided that $\lambda_f < 0.3$, the upper limit corresponding to the onset of skimming flow. From these fits to data, Macdonald showed that the attenuation coefficient a varies with the packing density of the cubes, and λ_f according to the approximately linear relationship $a = 9.6\lambda$. These data are shown in Fig. 5.

Also shown in Fig. 5 is the variation of a with λ_f obtained from the analytical exponential solution, which yields

$$a = h/l_s = h/(2l_c^2 L_c)^{\frac{1}{3}}, \tag{18}$$

where $l_c = s\kappa(h - d)$ and d is obtained from (12). Two curves are shown. When $s = 1$, so that the mixing length is continuous across the top of the canopy, the calculated values

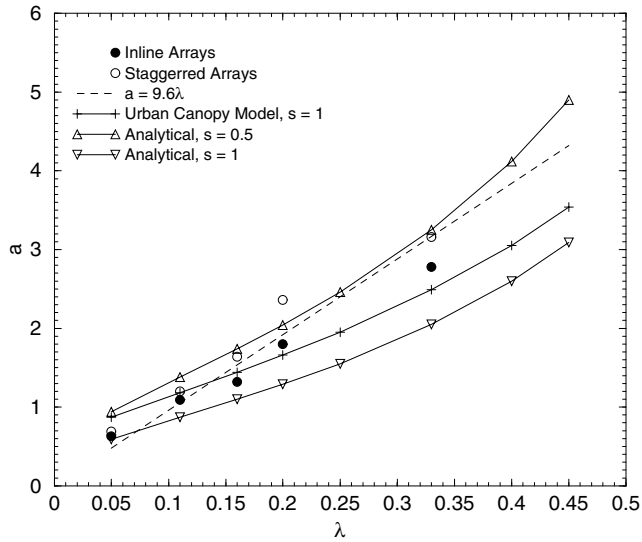

Figure 5. Attenuation coefficients a of exponential fits to wind profiles computed by urban canopy model (plus signs), compared with data measured by Macdonald *et al.* (1998) (circles), a best-fit straight line $a = 9.6\lambda$ to that data (dotted line), and with analytical model (up and down triangles).

of a are smaller than the observations. However, when $s = 1/2$, so that, as argued by Macdonald (2000), the mixing length within the canopy is one half the mixing length immediately above the canopy, then the values of a calculated from this exponential solution agree with the measurements much better.

Finally, also shown in Fig. 5 are the values of a obtained by fitting an exponential solution to the wind profiles shown in Fig. 4, which were computed from the full urban canopy model (with $s = 1$ and $\overline{c}_d = 2$). These values also agree reasonably well with the measurements. (Similar values obtained with $s = 1/2$ (not shown) do not agree well.) The urban canopy model agrees with the observations of a when $s = 1$ because the profiles from the urban canopy model are significantly different from the analytical exponential solution, mainly because for these values of λ_f the mixing length varies through most of the depth of the canopy (see Fig. 3), rather than being constant with height.

We conclude that the present urban canopy model gives reasonable agreement with the wind profiles measured by Macdonald for flow adjusted to the canopy, over the range of packing densities.

(*b*) *The effective roughness length of a canopy*

Measurements by Cheng and Castro (2002b) show that the spatially averaged flow above the canopy may be described by an effective roughness length z_0^{eff}, right down to the top of the roughness elements. Several methods have been proposed in the literature for obtaining this effective roughness length from the geometry and distribution of the roughness elements, with varying degrees of success (see e.g. Lettau 1969; Raupach 1992; Bottema 1996, 1997; Macdonald *et al.* 1998), as reviewed by Grimmond and Oke (1999). The urban canopy model is now used to calculate the effective roughness length, as it is clearly important that it yields good estimates for this parameter.

In the present approach, the canopy drag length-scale L_c is first computed as a function of roughness density using (5). The flow above such a canopy is then solved

numerically, and the effective roughness length z_0^{eff} extracted from the logarithmic portion of the mean velocity profile. This is therefore a two-tiered approach which first represents the obstacle array as a canopy, then solves for the flow over this canopy. Using this procedure, the urban canopy model is here validated against wind-tunnel data on roughness lengths of arrays of cubical obstacles (Hall *et al.* 1998). The drag and turbulent stress are parametrized as described in section 2. Based on the above estimation of the drag coefficient profile over cubes, a mean value of $\overline{c}_d = 2$ is used for the sectional drag coefficient. The turbulent stress is parametrized using the displaced mixing-length scheme. In this scheme, specification of d is necessary to close the model. The effective roughness is quite sensitive to the value of d and it is therefore important that reasonable values of d are used. Here, the empirical relationship of Macdonald *et al.* is used, as given by (12).

Lettau (1969) proposed a very simple empirical relationship relating the surface roughness z_0 of a group of obstacles of mean height h to its frontal area density λ_f :

$$z_0/h = 0.5\lambda_f. \tag{19}$$

This formula works well for low obstacle densities, but fails when λ_f increases beyond about 0.2. In particular, it predicts a linear increase of roughness with λ_f, whereas experimental data shows a peak in roughness at about $\lambda_f = 0.2$. Macdonald *et al.* (1998) developed a simple analytical model based on physical assumptions, and showed how Lettau's model could be generalized by incorporating the effect of obstacle density on the displacement height, using the empirical expression (12). Their expression for z_0 had the form

$$z_0/h = \left(1 - \frac{d}{h}\right) \exp\left[-\left\{\frac{C_{dh}}{2\kappa^2}\left(1 - \frac{d}{h}\right)\lambda_f\right\}^{-\frac{1}{2}}\right], \tag{20}$$

where κ is the von Karman constant. Using the value $C_{dh} = 1.2$, they obtained the curve shown in Fig. 6, which agrees very well with wind tunnel roughness data for cubes (Hall *et al.* 1996), also shown for comparison.

Using the same empirical expression for d given in (12), the roughness lengths computed by the present urban canopy model are also shown in Fig. 6. The comparison indicates that the urban canopy model predicts roughness lengths broadly in agreement with the experimental data and with the simple analytical model of Macdonald *et al.* In particular it faithfully reproduces the characteristic peak in z_0/h at the correct value of λ_f. In comparing these two models, we recall that the canopy approach adopted here incorporates a drag formulation which is defined over the whole depth of the canopy. Hence, it differs from the bulk drag approach adopted by Macdonald *et al.* We note, however, that the value of $\overline{c}_d = 2$ used here and the value of $C_{dh} = 1.2$ used by these authors are consistent with each other, since it was shown in the last section that a value of $\overline{c}_d = 2$ could be deduced from Cheng and Castro's measurements whilst they obtained a value of $C_{dh} = 1.1$ from the same dataset. The model of Macdonald *et al.* has been assessed as one of the better performing morphometric models for estimating roughness lengths for real urban areas in the recent review of Grimmond and Oke (1999). Hence, it is encouraging that the present urban canopy model gives comparable results to the method of Macdonald *et al.*

Figure 7 shows values of z_0/h obtained from these simulations plotted against the canopy parameter L_c/h. This curve also shows a peak in z_0/h. Given that the peak appears at a value of $L_c/h \approx 5$, canopies with this value of L_c/h have maximum non-dimensional roughness z_0/h and in this sense are optimally rough. The significance of

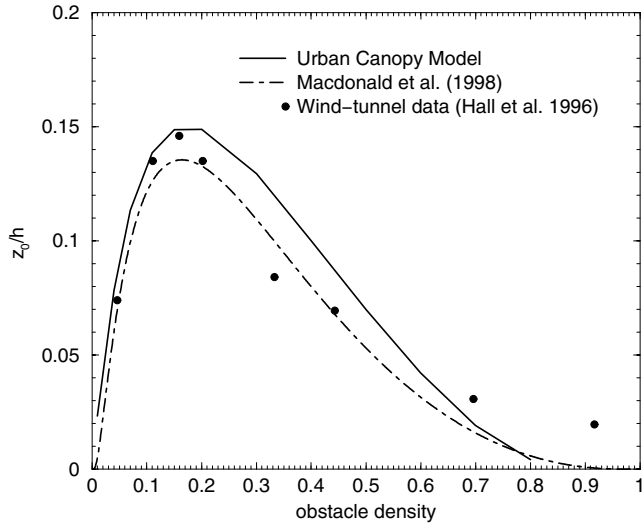

Figure 6. Roughness lengths z_0/h computed from the urban canopy model as a function of λ_f. Urban canopy model uses a value of $\overline{c}_d = 2$.

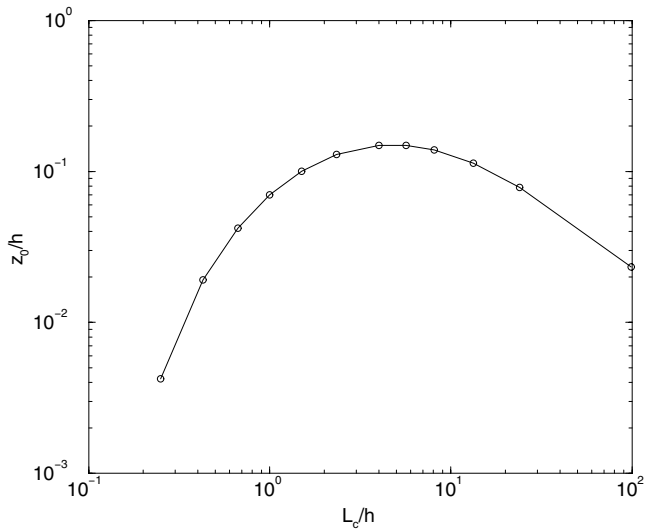

Figure 7. Roughness lengths z_0/h computed from the urban canopy model as a function of L_c/h (see text).

this curve is that it should apply to arrays with obstacles of any shape, not just cubes. This is in contrast to the z_0/h vs. λ_f curve, where one would expect a different curve for obstacles with a different aspect ratio, owing to different values of $\overline{c}_d$.

4. Adjustment of a Rural Boundary Layer to an Urban Canopy

In this section we consider the canonical problem of a logarithmic rural boundary layer adjusting to a homogeneous canopy of urban roughness elements. BJH developed a quasi-linear analytical model to consider this adjustment problem. They showed that,

above the canopy, z_0^{eff} varies smoothly with fetch through an adjustment region from the upstream roughness to the equilibrium roughness length of the canopy. BJH also presented analytical calculations and scaling arguments for the adjustment within the canopy. The analytical model of BJH is valid in the limit of a sparse canopy, when the canopy induces small perturbations to the rural wind profile. Here we perform fully nonlinear numerical simulations with the urban canopy model which are more generally applicable to sparse as well as denser canopies.

(*a*) *Adjustment of winds within an urban canopy*

BJH argue on the basis of scaling arguments motivated by linear analysis that L_c represents a length-scale for an incident wind profile to adjust to the canopy. They show that the wind adjusts on a length-scale of order x_0 given by the expression

$$x_0 \sim L_c \ln K, \tag{21}$$

where $K = (U_h/u_*)(h/L_c)$. Here h is the canopy height and U_h is the mean wind speed at the canopy top.

In the appendix, a different but related problem is considered which reinforces the dynamical significance of L_c as an adjustment length-scale. An initial perturbation to an equilibrium wind profile within a canopy is also shown to decay with a relaxation length-scale of L_c downstream of the perturbation. Although the dynamics of this problem are somewhat different from the first one it is interesting that L_c again plays the role of an adjustment length-scale, albeit under somewhat restrictive initial perturbations.

Here the adjustment problem is again addressed, this time using the present nonlinear urban canopy model. The scaling analysis of BJH is unable to give a value for the scaling coefficient in (21). Hence, numerical experiments are now performed to validate (21) and to compute the value of the scaling coefficient.

A number of numerical experiments are performed to simulate the nonlinear adjustment of an initially logarithmic rural wind profile to an urban-type canopy. Three of the runs, corresponding to $L_c = 18.4$, 13.1 and 7.8 m, are shown for illustration. The canopy height $h = 2.3$ m. This height was chosen to correspond to the height of the cubical obstacles used in the 'field' experiment of Davidson *et al.* (1995) discussed in section 4(b). Although this canopy height is clearly much smaller than typical urban building heights, the relevant dimensionless parameters, such as z_0/h used here do correspond to realistic values. Moreover, all results presented here are in dimensionless form. For each of these runs, vertical profiles of mean horizontal wind speed, non-dimensionalized by U_h, corresponding to fetches of L_c, $2L_c$, $3L_c$ and $4L_c$ from the leading edge of the canopy, are shown in Fig. 8. This figure shows that the adjustment is quite rapid, occurring within a few L_c. In Fig. 9 the ratio x_0/L_c is plotted against the log factor $\ln K$ appearing in (21). In computing $\ln K$, it is assumed that the incident wind profile is logarithmic, so that $U_h/u_* = 1/\kappa \ln(h/z_0)$, where z_0 is the upstream roughness length. The range of values shown in Fig. 9 corresponds to λ values of between 0.11 and 0.31, as encountered in typical urban areas. A linear fit to the five data points is also shown. It shows that, although there is some curvature apparent in the data, (21) holds reasonably well as a first approximation and gives a value for the scaling coefficient of approximately 3. As a rule of thumb, therefore, mean winds adjust within a distance

$$x_0 = 3L_c \ln K, \tag{22}$$

where the log factor varies between 0.5 and 2 for typical urban parameters. Note, however, that the log scaling must eventually break down for very sparse canopies, when

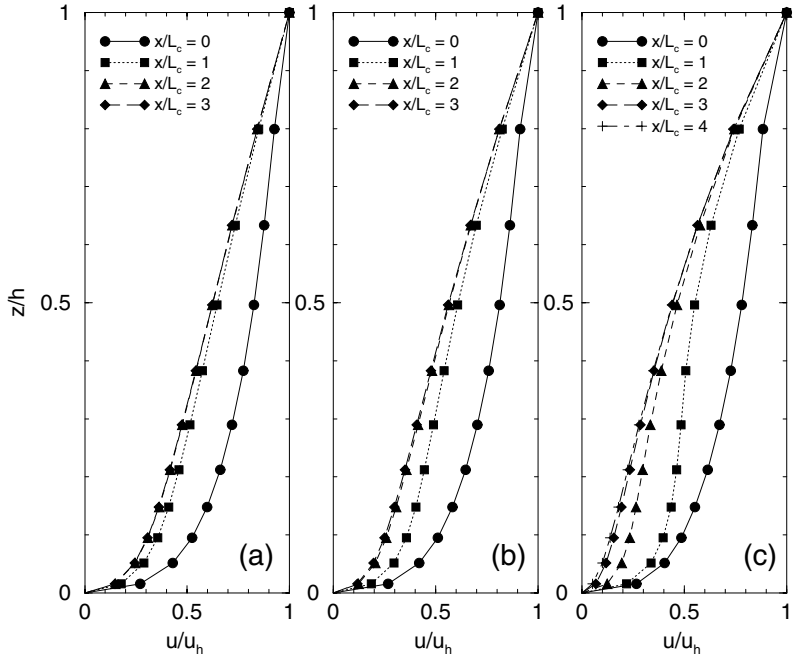

Figure 8. Adjustment of mean wind profile in a canopy for three different values of the canopy drag length-scale L_c: (a) 18.4 m, (b) 13.1 m and (c) 7.8 m. Mean wind speed is normalized by its value at the canopy top.

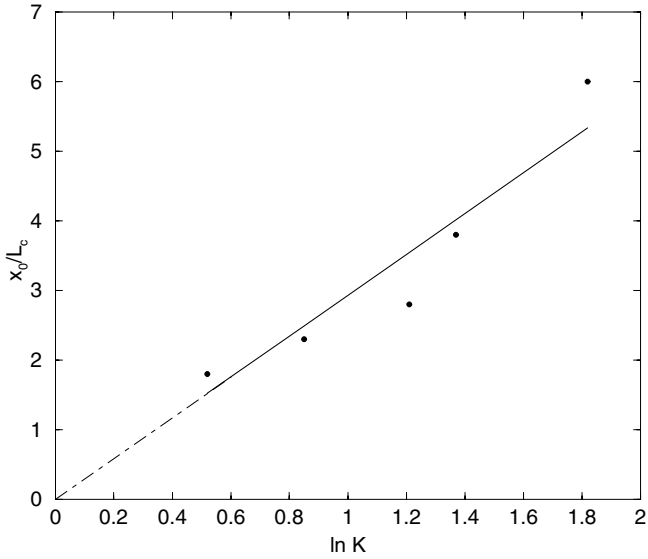

Figure 9. Variation of normalized adjustment distance x_0/L_c with canopy parameter ln K. See text for definition of symbols.

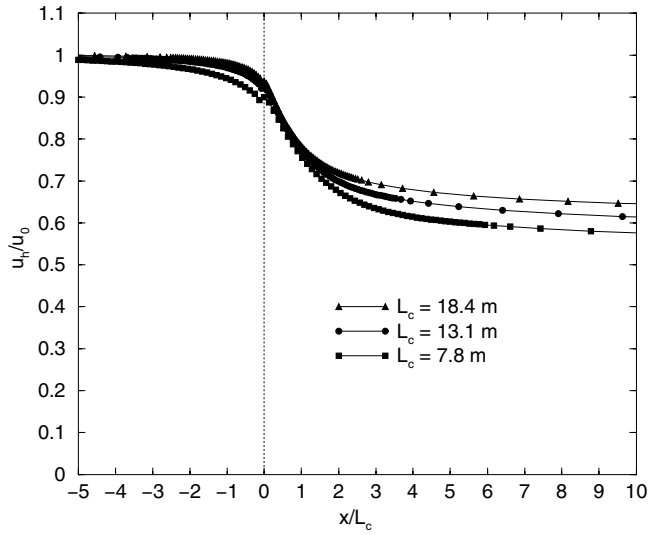

Figure 10. Evolution of mean wind speed at top of canopy U_h corresponding to the values of L_c of Fig. (8).

the parameter h/L_c becomes very small and ln K then becomes negative. Hence, care must be taken not to extrapolate (22) outside its range of validity. The length-scale x_0 then gives a dynamical length-scale to a neighbourhood: the urban morphology within a radius x_0 determines the local canopy winds.

We note that the relatively rapid adjustment described above pertains to the wind profile within the canopy normalized by U_h. However, U_h itself is proportional to the local friction velocity in the boundary-layer flow above once the flow in the canopy has adjusted. The wind at the top and above the canopy follows a much longer development as the boundary layer above adjusts to the new enhanced roughness of the urban area. This is indicated by the plots in Fig. 10, which show the development with fetch of the wind speed at the top of the canopy normalized by the upstream wind speed at the same height, U_h/U_0. These plots show a residual slow decrease in U_h/U_0 beyond $x > x_0$. Hence, the adjustment of the flow within the canopy is really an adjustment to the local turbulent stress at the top of the canopy, which is itself evolving slowly downwind.

(*b*) *The adjustment number* N_c

It has been common practice in the literature to quantify wind adjustment through a regular array in terms of the number of rows. It is proposed here that L_c is a better way of characterizing the adjustment. It may be misleading to quote adjustment distances as a given number of rows because that number will be different for arrays of different obstacle densities. Nevertheless, it is sometimes useful to estimate roughly the number of rows for mean winds to adjust through a regular array. This is here done for the case of a cubical array as a function of the obstacle density. Consider cubes of side h separated by a distance w in an aligned array, where w is the total separation, including the width of the obstacles. Then L_c is given by (5) as

$$L_c/h = \frac{2}{\overline{c}_d}\left(\frac{1-\lambda}{\lambda}\right), \tag{23}$$

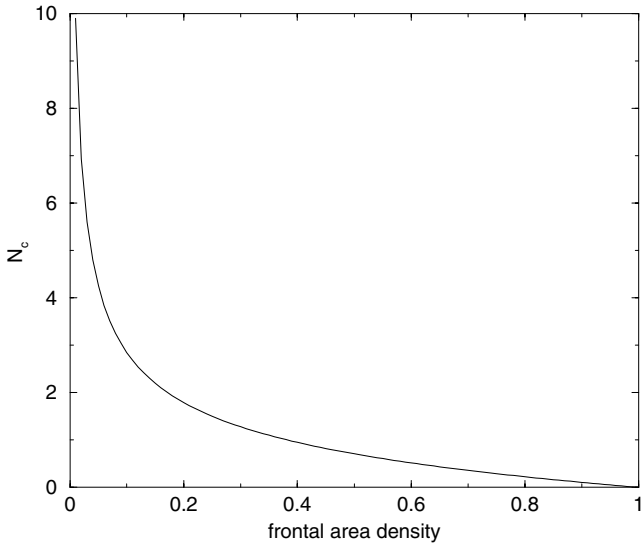

Figure 11. Variation of adjustment number N_c with obstacle density λ for a cubical array (using $\overline{c}_d = 2$). See text for explanation.

where $\lambda = \lambda_f = \lambda_p = (h/w)^2$. Defining a new dimensionless adjustment parameter $N_c \equiv L_c/w$, we find

$$N_c = \frac{2}{\overline{c}_d}\left(\frac{1}{\sqrt{\lambda}} - \sqrt{\lambda}\right). \tag{24}$$

The number of rows for the mean wind to adjust is then given by $3N_c \ln K$. Figure 11 shows a plot of N_c as a function of λ for $\overline{c}_d = 2$. Macdonald *et al.* (2000) performed wind tunnel simulations with arrays of cubes with, e.g. $\lambda = 0.16$, and $h/z_0 \approx 40$. These figures imply that the flow is adjusted after $3N_c \ln K \approx 2$ rows. This agrees with the measurements of Macdonald *et al.* (2000), who observed little change in vertical profiles of mean horizontal velocity within arrays after the second row.

(*c*) *Wind deceleration through a canopy*

Results from the urban canopy model are now compared with the measurements of Davidson *et al.* (1995, 1996), who performed two sets of experiments using staggered arrays of obstacles as shown in Fig. 12. The first was a field experiment with obstacle dimensions $w \times b \times h = 2.2$ m $\times$ 2.45 m $\times$ 2.3 m, while the second was a wind tunnel boundary-layer experiment with $w = b = h = 0.12$ m. Both experiments were conducted under conditions of neutral stratification. The incident wind profile was logarithmic, with $z_0 = 11$ mm, $u_* = 0.49$ m s^{-1} (field) and $z_0 = 0.4$ mm, $u_* = 0.21$ m s^{-1} (wind tunnel). The obstacle density $\lambda_f = \lambda_p$ was equal to 0.11. Davidson *et al.* measured the time-mean streamwise velocities at half canopy height at several locations in the cross-stream direction. Lateral averages were computed and are used here as measures of the spatially averaged wind (Fig. 12).

Figure 13 shows the streamwise variation of U at half the obstacle height obtained from the urban canopy model, together with comparisons with the measurements of Davidson *et al.* (1995, 1996) and the quasi-linear model of BJH. The parameters used in the simulations were taken from the field experiment only, since the results from the wind tunnel collapse onto these when non-dimensionalized as in Fig. 13. This collapse

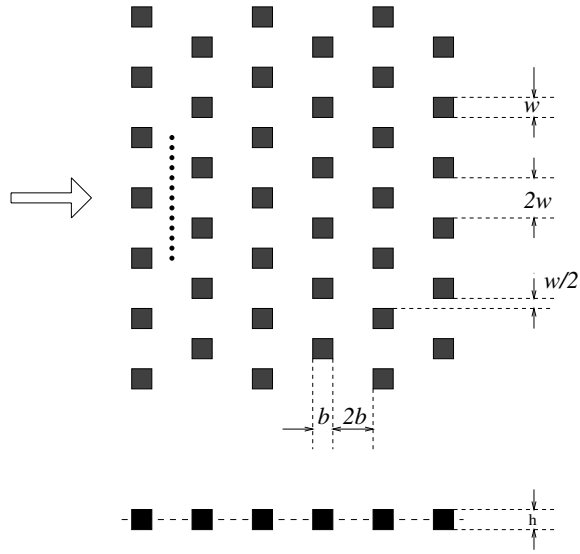

Figure 12. Array of obstacles used in the experiments of Davidson *et al.* (1995, 1996). A side view is shown below a plan view. Dots indicate the position of measurements.

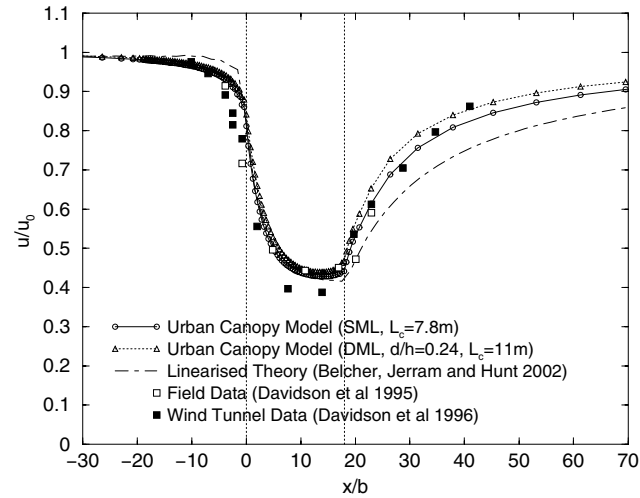

Figure 13. Deceleration of mean wind at half the roughness element height through canopy of roughness elements. Comparison of the urban canopy model with the measurements of Davidson *et al.* (1995, 1996). The canopy lies between $x/b = 0$ and 18; b is defined in Fig. 12.

occurs because the relevant dimensionless parameters, namely h/L, L/L_c and z_0/h (where L is the total length of the canopy and h is its height) are approximately the same in both experiments. Hence the simulations have $h = 2.3$ m, $L = 44.1$ m and an incident logarithmic velocity profile with $u_* = 0.49$ m s^{-1} and $z_0 = 0.011$ m. The obstacle density $\lambda_p = 0.11$, so that (12) yields $d/h = 0.24$.

The canopy drag length-scale L_c was tuned to give the best fit. With the mixing-length scheme of the urban canopy model, (11), (12) and (13), this tuning yields $L_c = 11$ m. For this choice of parameters, the urban canopy model gives good agreement

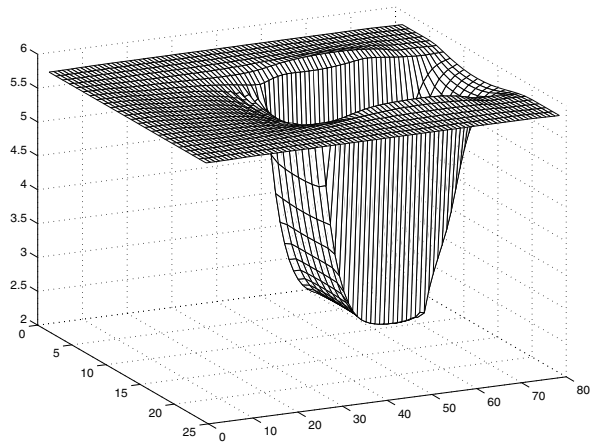

Figure 14. Surface plot of spatially averaged mean wind speed at half canopy height through the Davidson *et al.* (1995, 1996) array. Vertical axis: wind-speed U (m s^{-1}); horizontal axes: streamwise and lateral position.

with the data. The overall shape of the deceleration curve is captured throughout. Also shown in Fig. 13 is the corresponding curve from the quasi-linear theory of BJH, which employed the simple mixing length scheme, namely $l_{\mathrm{m}} = \kappa z$, with the value of $L_{\mathrm{c}} = 7.8$ m. For direct comparison a numerical simulation employing the simple mixing-length scheme with the same value of $L_{\mathrm{c}} = 7.8$ m is also shown. There is excellent agreement between the nonlinear urban canopy model and the quasi-linear theory within the canopy. The quasi-linear model underpredicts the wind speed in the recovery region beyond the canopy, however.

The value of $L_{\mathrm{c}} = 11$ used here with the urban canopy model corresponds to $\overline{c}_d = 3.3$. This value is smaller than the value of $\overline{c}_d = 4.7$, which corresponds to $L_{\mathrm{c}} = 7.8$, required to give good agreement with the simple mixing-length model. The reason is that the mixing-length model in the urban canopy model yields greater mixing and so the wind speed at $z = h/2$ is reduced to a level in agreement with the observations for a smaller value of $\overline{c}_d$. Nevertheless, $\overline{c}_d = 3.3$ is higher than the mean value of 2 obtained from measurements in section 2(b), although it is not far outside the expected range of 2–3.

Close examination of Fig. 13 reveals that, at the leading edge of the canopy, $x = 0$, the urban canopy model gives $U/U_0 \approx 0.85$, whereas the measurements from the field experiment give $U/U_0 \approx 0.7$. BJH argue that the deceleration at the leading edge of the canopy is enhanced by the finite volumes of the canopy elements displacing streamlines over and around the canopy elements, yielding a substantial dispersive stress. We interpret the large value of $\overline{c}_d$ as being at least partly due to the blocking effect by the large canopy elements, which is also responsible for the large velocity reduction at the leading edge of the canopy as indicated by the data in Fig. 13. It seems likely that a quantitative model incorporating this 'finite volume effect' as well as the drag force would yield good agreement with the data with a smaller, and perhaps more physically plausible, value of $\overline{c}_d$.

Comparisons between two-dimensional (2D) and 3D simulations show that the spatially averaged flow along the axis of the canopy is essentially 2D, so that the lateral size of the canopy itself plays no significant role as far as the mean flow within the bulk of the canopy is concerned. The essentially 2D structure of the 3D flow is evident from the surface plot in Fig. 14. Here the spatially averaged mean wind at half canopy height

is plotted as a function of both streamwise fetch and lateral distance. Sections through this plot parallel to the streamwise axis at different lateral positions would appear very similar, showing that there is little lateral variation in the mean wind-speed within the canopy.

5. Conclusions

We have developed an urban canopy model to calculate the spatially averaged mean winds within and above urban areas. The spatial averaging approach inherent in the canopy formalism provides a natural way of handling the inhomogeneity of urban areas, which presents serious conceptual and computational difficulties to other approaches. The urban canopy model captures the variations in the spatially averaged mixing and transport induced by changes in density and type of urban roughness elements, such as in passing from rural to suburban to fully urban surfaces. The formal averaging procedure upon which the urban canopy model is based is the same as that involved in plant canopies. However, important differences exist in the way the drag and mixing are parametrized. Particular care is taken to develop parametrizations which reflect the differences between urban and vegetation canopies, and which take into account the fact that buildings are large obstacles. This distiguishes the present urban canopy model both from vegetation canopy models and other urban canopy models in the literature. The urban roughness elements are represented by a canopy-element drag which is computed from their morphological parameters and a mean sectional drag coefficient. The value of the drag coefficient used is important; it is here derived from experimental data for turbulent shear flow over surface-mounted cubes. Turbulent mixing is represented using a mixing-length model with a mixing length that depends upon the density of the canopy and distance from the ground, which captures processes known to occur in canopies. Unlike vegetation, urban canopies are not 'deep'. Hence, the mixing length is not constant with height in the canopy. This has the effect that vertical profiles of spatially averaged mean velocity are not exponential in urban canopies.

An attractive feature of the urban canopy model is that only a few parameters are needed to initialize it, namely the morphological parameters λ_f, λ_p and h, and the mean drag coefficient $\overline{c}_d$. The parameters λ_f, λ_p and h, are relatively straightforward to estimate (see e.g. Grimmond and Oke 1999). Experimental measurements of $c_d(z)$ for a variety of obstacle densities and arrangements are not currently available, but based on existing data we believe that the mean coefficient $\overline{c}_d$ is sufficiently constrained, and recommend a value of 2 for modelling urban areas. The urban canopy model is sufficiently simple that it can be implemented in NWP.

The urban canopy model compares well with wind tunnel and field measurements of the profiles of spatially averaged wind above and within regular arrays of cubical obstacles. These comparisons offer strong evidence that the basic canopy approach is appropriate for modelling the spatially averaged flow through the groups of large-scale roughness elements that make up urban areas.

An aspect of urban areas that significantly complicates both measurement and modelling is the heterogeneity over a range of length-scales. Although the canopy approach involves averaging over short scales, it can resolve the response of the spatially averaged flow to changes in the density and type of roughness elements. Hence we have used the present fully nonlinear urban canopy model to study the canonical problem of adjustment of a rural boundary layer to an urban canopy. Numerical simulations support the scaling proposed by BJH for the distance x_0, required for the wind profile within the canopy to adjust to the urban canopy, and suggest that

$$x_0 = 3L_c \ln K, \tag{25}$$

where $\ln K$ depends weakly on canopy parameters and varies between 0.5 and 2. Hence the density and type of roughness elements within a radius x_0 affect the local winds within the urban canopy. In this sense x_0 provides a dynamical definition of a neighbourhood.

The present urban canopy model and the quasi-linear model of BJH agree well with the measurements taken by Davidson *et al.* (1995, 1996) of adjustment of a rural boundary layer to an urban canopy, but only when they have larger values of the drag coefficient than the range of values of 2–3 estimated from measurements. The nonlinear urban canopy model, which has a more complete mixing-length parametrization, requires a value of 3.3, whereas the quasi-linear model of BJH requires an even larger value of 4.7. Whilst the value of 3.3 is only a little higher than the measured range, the measurements indicate that the wind decelerates more upwind of the canopy than suggested by the urban canopy model. Following BJH we attribute this deceleration to streamline deflection caused by the large volumes of the large-scale urban roughness elements. This streamline deflection then yields a dispersive stress upwind of the canopy that decelerates the spatially averaged wind. Hence, although the dispersive stress is probably small once the flow has adjusted to the canopy, it is large just upwind of a canopy, or in the vicinity of isolated large buildings. It remains an important task for future work to incorporate this process into the urban canopy model.

Acknowledgements

Thanks are due to Hong Cheng and Robert Macdonald for making their wind tunnel data available to us, and for useful discussions. We also thank Tim Oke, Andy Brown, Gabriel Rooney, Hong Cheng and Ian Harman for helpful comments on earlier drafts of this paper. The BLASIUS model was kindly supplied by Andy Brown and Nigel Wood at the Met Office. Marc Stringer provided valuable programming support. O.C. gratefully acknowledges funding from the Universities Weather Research Network and the Natural Environment Research Council, grant number DST/26/39. This work forms part of the UWERN Urban Meteorology Programme.

Appendix A

Decay of perturbations to an equilibrium profile within a canopy

In this appendix, we consider perturbations of an equilibrium wind profile within a canopy and investigate how they decay with distance downstream. To simplify the analysis, it is assumed that the canopy is homogeneous and two-dimensional. The equations of motion for the perturbations can be derived from the momentum and continuity equations for the full spatially averaged fields U and W by writing, for example $U = U_0 + u$. The equations for the perturbed quantities are then linearized by neglecting products of perturbation quantities. Using units such that the fluid density $\rho = 1$, this gives the following equations:

$$U_0\frac{\partial u}{\partial x} + w\frac{\partial U_0}{\partial z} + \frac{\partial p'}{\partial x} = \frac{\partial \tau'}{\partial z} - D', \tag{A.1}$$

$$U_0\frac{\partial w}{\partial x} + \frac{\partial p'}{\partial z} = \frac{\partial \tau'}{\partial x}, \tag{A.2}$$

$$\frac{\partial u}{\partial x} + \frac{\partial w}{\partial z} = 0, \tag{A.3}$$

where U_0 is the unperturbed equilibrium horizontal wind velocity, and u, w, τ', p' and D' are the perturbations from the equilibrium values of the mean horizontal velocity, vertical velocity, stress, pressure and drag force respectively. The pressure can be eliminated from the above equations to give

$$U_0\left(\frac{\partial^2 w}{\partial z^2}+\frac{\partial^2 w}{\partial x^2}\right)-U_0''w=\frac{\partial D'}{\partial z}+\frac{\partial^2\tau'}{\partial x^2}-\frac{\partial^2\tau'}{\partial z^2}. \tag{A.4}$$

With the stress and drag force parametrized by $\tau = l_{\mathrm{m}}^2\,(\partial U/\partial z)^2$ and $D = U^2/L_{\mathrm{c}}$, respectively, the perturbations τ' and D' are given by

$$\tau' = 2l_{\mathrm{m}}^2\frac{\partial U_0}{\partial z}\frac{\partial u}{\partial z}, \tag{A.5}$$

$$D' = 2U_0u/L_{\mathrm{c}}. \tag{A.6}$$

If we assume that the initial equilibrium profile $U_0(z)$ is exponential within the canopy (see section 4), being given by

$$U_0(z) = U_h\exp\{a(z/h-1)\}, \tag{A.7}$$

and that the initial perturbation is simply proportional to U_0,

$$u(0,\,z) = \epsilon U_0(z), \tag{A.8}$$

then (A.4) has a solution which decays exponentially with distance x downstream of the perturbation:

$$u(x,\,z) = u(0,\,z)\exp(-x/L_{\mathrm{c}}), \tag{A.9}$$

with a characteristic e-folding length-scale of magnitude L_{c}.

This simple result indicates that the parameter L_{c} acts as some kind of adjustment length-scale, and reinforces the conclusions arrived at on the basis of scaling analysis in BJH and the numerical simulations presented in the present paper.

References

Batchelor, G. K. 1967 *An introduction to fluid dynamics*. Cambridge University Press

Belcher, S. E., Jerram, N. and Hunt, J. C. R. 2003 Adjustment of the atmospheric boundary layer to a canopy of roughness elements. *J. Fluid Mech.*, **488,** 369–398

Bohm, M., Finnigan, J. J. and Raupach, M. R. 2000 'Dispersive fluxes in canopy flows: Just how important are they?'. Pp. 106–107 in Proceedings of 24th conference on agricultural and forest meteorology, 14–18 August 2000, Davis, CA, USA. American Meteorological Society, 45 Beacon Street, Boston MA02108-3693, USA

Bottema, M. 1996 Roughness parameters over regular rough surfaces: Experimental requirements and model validation. *J. Wind Eng. Indust. Aero.*, **64,** 249–265

1997 Urban roughness modelling in relation to pollutant dispersion. *Atmos. Environ.*, **31,** 3059–3075

Britter, R. E. and Hanna, S. R. 2003 Flow and dispersion in urban areas. *Ann. Rev. Fluid Mech.*, **35,** 469–496

Brown, M. 2000 'Urban parameterisations for mesoscale meteorological models'. Chap. 5 in *Mesoscale atmospheric dispersion*. Ed. Z. Boybeyi. Wessex Press

Cheng, H. and Castro, I. P. 2002a Near wall flow development after a step change in surface roughness. *Boundary-Layer Meteorol.*, **105,** 411–432

2002b Near wall flow over urban-like roughness. *Boundary-Layer Meteorol.*, **104,** 229–259

Cionco, R. M. 1965 A mathematical model for air flow in a vegetative canopy. *J. Appl. Meteorol.*, **4,** 517–522

Craig, K. J. and Bornstein, R. D. 2002 'Urbanisation of numerical mesoscale models'. Pp. 17–30 in abstracts from workshop on urban boundary layer parameterisations, 24–25 May 2001, Zurich, Switzerland. COST Action 715, ISBN 92-894-4143-7

Davidson, M. J., Mylne, K., Jones, C., Phillips, J., Perkins, R., Fung, J. and Hunt, J. C. R. 1995 Plume dispersion through large groups of obstacles—a field investigation. *Atmos. Environ.*, **29,** No. 22, 3245–3256

Davidson, M. J., Snyder, W. H., Lawson, R. E. and Hunt, J. C. R. 1996 Wind tunnel simulations of plume dispersion through groups of obstacles. *Atmos. Environ.*, **30,** No. 22, 3715–3731

ESDU 1986 Mean fluid forces and moments on rectangular prisms: Surface-mounted structures in turbulent shear flow. Engineering Sciences Data Item Number 80003. ESDU International, 27 Corsham St., London N1 6UA

Finnigan, J. J. 1985 'Turbulent transport in flexible plant canopies'. Pp. 443–480 in *The forest–atmosphere interaction*. Eds. B. A. Hutchinson and B. B. Hicks. Reidel, Dordrecht

2000 Turbulence in plant canopies. *Ann. Rev. Fluid Mech.*, **32,** 519–572

Finnigan, J. J. and Belcher, S. E. 2003 Flow over a hill covered with a plant canopy. *Q. J. R. Meteorol. Soc.*, **130,** 1–29

Grimmond, C. S. B. and Oke, T. R. 1999 Aerodynamic properties of urban areas derived from analysis of surface form. *J. Appl. Meteorol.*, **38,** 1262–1292

Hall, D. J., Macdonald, R., Walker, S. and Spanton, A. M. 1998 'Measurements of dispersion within simulated urban arrays—a small scale wind tunnel study.' *BRE Client Report CR244/98.* Building Research Establishment, Garston, Watford WD25 9XX

Lettau, H. 1969 Note on aerodynamic roughness-parameter estimation on the basis of roughness-element description. *J. Appl. Meteorol.*, **8,** 828–832

Macdonald, R. W. 2000 Modelling the mean velocity profile in the urban canopy layer. *Boundary-Layer Meteorol.*, **97,** 25–45

Macdonald, R. W., Griffiths, R. F. and Hall, D. J. 1998 An improved method for the estimation of surface roughness of obstacle arrays. *Atmos. Environ.*, **32,** No. 11, 1857–1864

Macdonald, R. W., Carter, S. and Slawson, P. R. 2000 'Measurements of mean velocity and turbulence statistics in simple obstacle arrays at 1:200 scale.' *Thermal Fluids Report 2000-01.* University of Waterloo

Martilli, A., Clappier, A. and Rotach, M. W. 2002 An urban surface exchange parameterisation for mesoscale models. *Boundary-Layer Meteorol.*, **104,** 261–304

Panofsky, H. A. and Dutton, J. A. 1984 *Atmospheric turbulence*. John Wiley and sons, Chichester

Raupach, M. R. 1992 Drag and drag partition on rough surfaces. *Boundary-Layer Meteorol.*, **60,** 375–395

Raupach, M. R. and Shaw, R. H. 1982 Averaging procedures for flow within vegetation canopies. *Boundary-Layer Meteorol.*, **22,** 79–90

Raupach, M. R., Finnigan, J. J. and Brunet, Y. 1996 Coherent eddies and turbulence in vegetation canopies: The mixing layer analogy. *Boundary-Layer Meteorol.*, **78,** 351–382

Vardoulakis, S., Fisher, B. E. A., Pericleous, K. and Gonzalez-Flesca, N. 2003 Modelling air quality in street canyons: A review. *Atmos. Environ.*, **37,** 155–182

Wood, N. 1992 'Turbulent flow over three-dimensional hills'. PhD dissertation, Reading University

Wood, N. and Mason, P. J. 1993 The pressure force induced by neutral, turbulent flow over hills. *Q. J. R. Meteorol. Soc.*, **119,** 1233–1267

Wooding, R. A., Bradley, E. F. and Marshall, J. K. 1973 Drag due to regular arrays of roughness elements. *Boundary Layer Meteorol.*, **5,** 285–308